CHEMNANOMAT

CHEMISTRY OF NANOMATERIALS FOR ENERGY, BIOLOGY AND MORE

www.chemnanomat.org

Accepted Article

Title: Correlating catalyst structure and activity at the nanoscale

Authors: Jordi Van Loon, Alexey V. Kubarev, and Maarten B.J. Roeffaers

To be cited as: *ChemNanoMat* 10.1002/cnma.201700301

Link to VoR: http://dx.doi.org/10.1002/cnma.201700301

A Journal of

ACES Asian Chemical Editorial Society

A sister journal of **Chemistry – An Asian Journal** and **Asian Journal of Organic Chemistry**

WILEY-VCH

ChemNanoMat

10.1002/cnma.201700301

WILEY-VCH

FOCUS REVIEW

Correlating catalyst structure and activity at the nanoscale

Jordi Van Loon,[a] Alexey V. Kubarev,[a] and Maarten B. J. Roeffaers*[a]

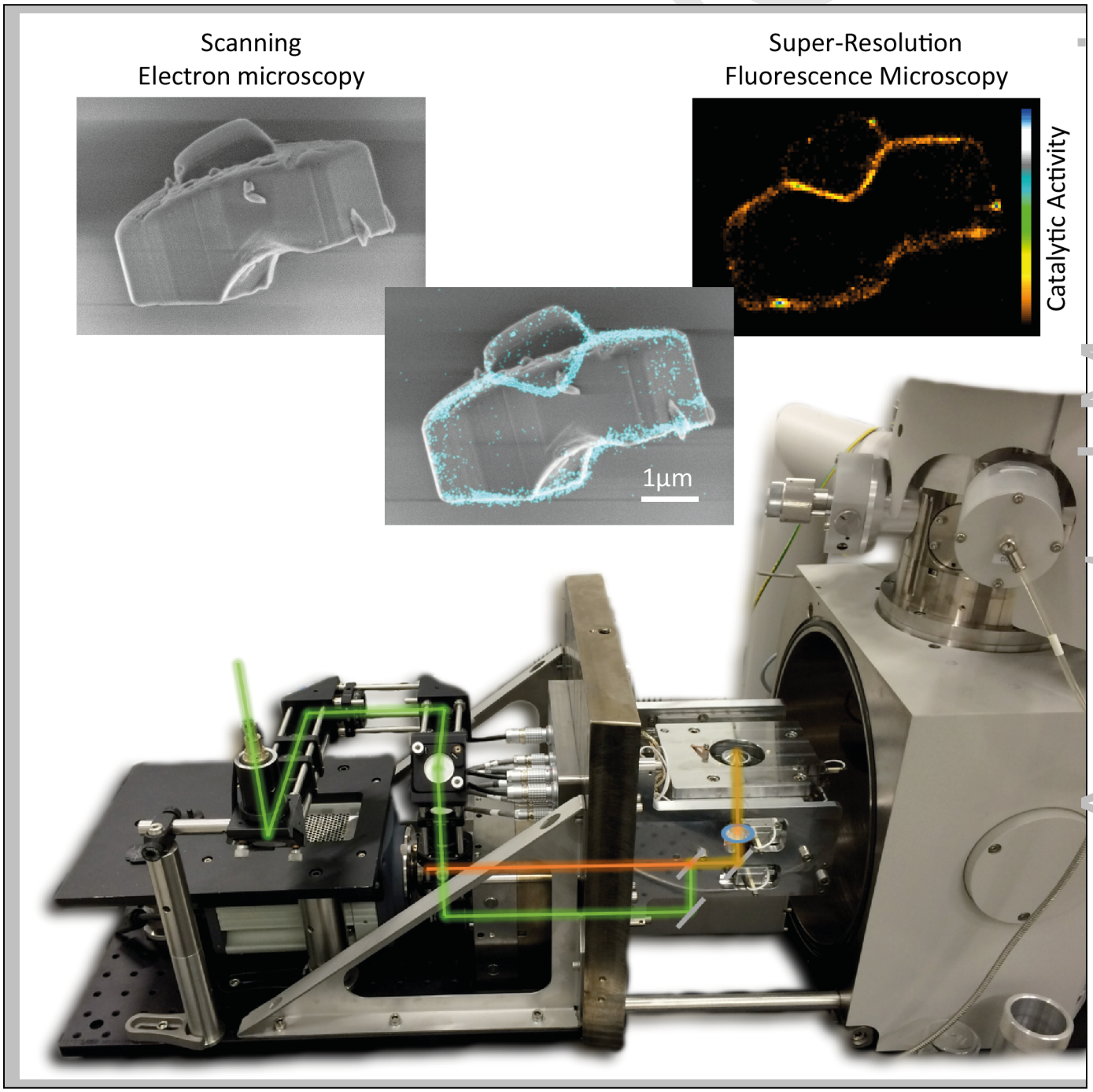

Abstract: Heterogeneous catalysts are commonly applied to enhance chemical reactions. Their performance is largely determined by catalyst structure and composition. These properties are however intrinsically variable at the nanoscale. Traditional bulk-scale characterization tools often fail to capture the structure-activity relationship at this scale. The development of fluorescence based assays has enabled catalytic activity mapping at the level of single catalytic turnovers, allowing catalyst activity to be investigated beyond the single particle level. Nonetheless, interpretation of these insights remains challenging without matching local structural information. This has resulted in increased efforts to develop approaches that correlate super-resolution fluorescence with electron microscopy. In this focus review, a concise overview of currently available approaches is provided, followed by some case studies in which correlative nanoscale structure-activity investigations of (photo)catalyst materials were performed.

1. Introduction

Over 80% of industrial scale chemical processes make use of heterogeneous solid catalysts,[1,2] such as supported metal nanoparticles (NP), metal oxides or zeolites, which speed up liquid or gas phase reactions.[3–9] The performance of these materials is largely determined by their structure, surface area, and chemical composition.[10,11] The intrinsic structural and compositional complexity often leads to significant variability in physicochemical properties and thus in catalytic activity on both the inter- and intraparticle level.[12–14] Consequently, the rational improvement of heterogeneous catalysts requires a thorough understanding of the structure-activity relationship down to the smallest possible length scales. This information cannot be obtained using traditional bulk scale characterization tools, as they yield ensemble averaged information. Highly resolved microscopy techniques, such as electron microscopy (EM) and scanning probe microscopy (SPM), allow nano and even atomic scale investigations of the catalyst structure. However, the structural heterogeneity renders it impossible to directly link these results to the corresponding catalytic performance since the latter information is only available from bulk scale activity testing.[15–17] The development of super-resolution fluorescence microscopy (SRFM) has recently enabled the investigation of catalyst activity down to the nanoscale with the possibility of resolving individual catalytic turnovers.[18–21] In such studies a fluorogenic reagent is used, *i.e.*, a non-fluorescent reagent that is catalytically converted into fluorescent product molecules. Some of these reaction products can even be detected with single molecule sensitivity and subsequently localized with nanometer-scale accuracy; note that the accuracy depends on several factors such as number of collected photons, signal-to-noise ratio, pixel size, etc.[22–24] This approach enabled the reconstruction of nanometer scale catalytic activity maps based on individual catalytic turnovers and revealed large inter- and intraparticle variations in activity distribution for various solid catalytic materials.[13,14,17,23,25,26] Nonetheless, insights into the structure-activity relationship remain limited, as nanoscale activity maps could not straightforwardly be related to the corresponding structural or compositional information. Commonly, this relationship was determined by linking activity maps to diffraction-limited optical transmission images of the same particle or highly-resolved electron micrographs obtained from similar crystals of the same synthesis batch.[27] Increased efforts have therefore been undertaken to combine SRFM and EM, and correlate information from both methods. This focus review has the goal to summarize benchmark efforts undertaken to investigate the structure-activity relationship in heterogeneous catalysts at the (sub)single-particle level.

[a] Dr. J. Van Loon, Dr. Alexey V. Kubarev, Prof. M.B.J. Roeffaers
Centre for Surface Chemistry and Catalysis, KU Leuven
Celestijnenlaan 200F, 3001 Leuven, Belgium
E-mail: maarten.roeffaers@kuleuven.be
Website: www.roeffaers-lab.org

Dr. Jordi Van Loon obtained his MSc in chemistry at the KU Leuven, Belgium in 2013. Afterwards, he joined the research group of Prof. Roeffaers as a doctoral researcher on the development of an integrated light and electron microscope to investigate the structure-activity relationship in heterogeneous catalyst samples. He obtained his PhD in 2017.

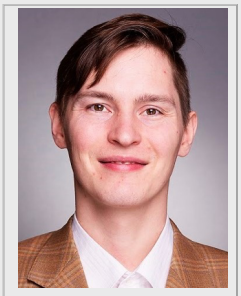

Dr. Alexey V. Kubarev obtained his MSc in chemistry at the Lomonosov Moscow State University, Russia in 2009. In 2013 he joined the research group of Prof. Roeffaers as a doctoral researcher on the development and application of fluorescence microscopy tools for in situ catalyst characterization. He has obtained his PhD in 2017.

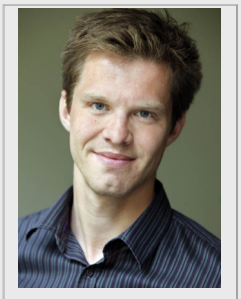

Professor Maarten B.J. Roeffaers obtained his PhD at the KU Leuven, Belgium in 2008 and conducted a postdoc at Harvard University, USA. Currently he is an associate professor at COK at the KU Leuven. In 2010, he started his own research group (www.roeffaers-lab.org) focusing on the development of optical microscopy tools to study heterogeneous catalysis and materials for sustainable chemistry. Amongst others, he was awarded an ERC starting grant (2012) and received the biennial ExxonMobil Chemical European Science and Engineering Award (2015).

2. Experimental strategies to combine electron and fluorescence microscopy

The SRFM assays used in catalysis research have been largely borrowed from biological research. The same applies to correlative fluorescence microscopy (FM) and EM studies that are used to determine the catalyst structure-activity relationship. Information from both microscopy modalities can be acquired by a correlative approach or using an integrated device, and EM is either achieved by scanning electron microscopy (SEM) or (scanning) transmission electron microscopy ((S)TEM). Choosing between these combinations has implications on the sort of experiments that can be performed. The catalyst under investigation and the catalytic process of interest thus dictate which approach is preferred.

2.1 Correlative light and electron microscopy

In correlative light and electron microscopy (CLEM) (Figure 1a), FM and EM are performed consecutively by employing dedicated microscopes. This allows full flexibility over the FM configuration, even enabling SRFM, but requires sample transfer which could lead to contamination and complicates image registration.[28,29] Fiducial markers, visible in both FM and EM, are commonly mixed into the sample to facilitate the image registration process. However, these markers might compromise sample integrity and it remains time consuming to accurately retrieve the region of interest (ROI) and perform image overlay. Alternatively, commercial systems have been developed that make use of a shuttle and find approach to enable an automated ROI retrieval. This procedure facilitates FM and EM correlation by means of a dedicated sample holder and a semi-automated calibration procedure. When TEM is used in a correlative approach, also the typical exhaustive sample preparation needs to be taken into consideration. This potentially introduces artefacts.

2.2 Integrated light and electron microscopy

Integrated light and electron microscopy (ILEM) can be based on both SEM and (S)TEM (Figure 1b and c), and, as two imaging modalities are combined into one, it has the potential to largely reduce sampling time and minimize the chances of sample contamination.[30,31] However, (S)TEM image formation is done via a detector placed coaxially to the electron gun. The objective lens of an epifluorescence microscope, therefore needs to be positioned at a 90-degree angle. This necessitates sample rotation when switching between modalities and implies that only consecutive experiments can be performed. Additionally, due to these geometrical constraints, a long working distance objective lens is required, which only allows diffraction-limited confocal laser scanning microscopy (CLSM). Due to this discrepancy in resolving power between TEM and CLSM, it is typically sufficient to perform qualitative image registration which does not require the use of fiducial markers.[30] In an SEM based ILEM, the objective lens and electron gun can be placed at opposite sides of the sample. This allows simultaneous SRFM and SEM. To study the catalyst under realistic conditions, the sample needs to be submerged inside a liquid environment. As such liquid contained samples are not compatible with the high vacuum conditions of the EM. This complicates the application of ILEM to correlate catalyst structure to activity at the nanoscale. Similar to biological experiments this can be overcome with specialized sample holders.[32]

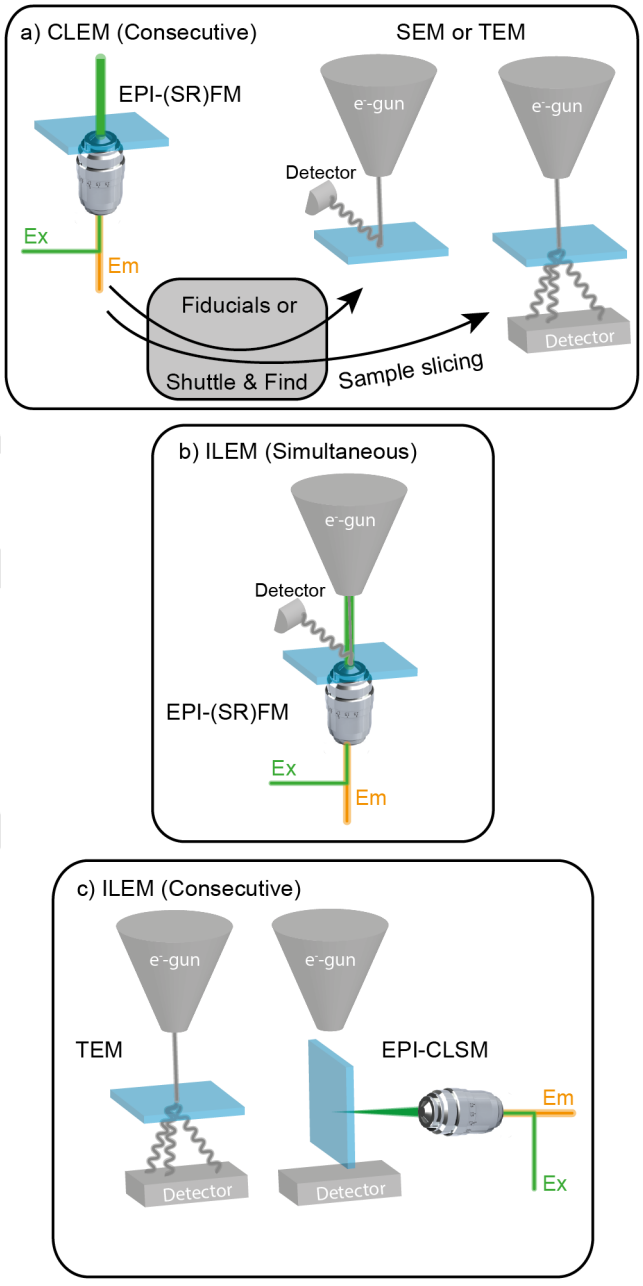

Figure 1. Schematic representation of the different approaches to correlate catalyst structure and activity on the nanoscale by means of FM and EM. a) Correlative light and electron microscopy (CLEM), enables consecutive (SR)FM and SEM or TEM, but requires fiducial markers or a shuttle and find approach to facilitate ROI retrieval and in case of TEM, additional sample slicing is required. b) Integrated light and electron microscopy (ILEM) that combines wide-field FM with SEM or c) confocal laser scanning microscopy (CLSM) with

TEM. Whereas the former allows a simultaneous use of both modalities, the latter only allows consecutive imaging due to its intrinsic configuration.

3. Correlating catalyst structure and activity

3.1 Nanoscale structure-activity investigation of metal nanoparticles

The catalytic activity of metal nanoparticles (NP's) is determined by the presence of active surface sites which is closely related to the expression of specific crystallographic facets, defects or influences from the support.[10] Due to intrinsically small dimensions of NP's, EM has been indispensable from the initial SRFM investigations to provide structural information that complements the catalytic performance.[20] However, in these studies, pioneered by Chen and co-workers, metal NP catalysts are commonly coated with a mesoporous silica shell to stabilize their morphology and prevent aggregation. This shell additionally facilitates SRFM as the diffusion of fluorescent product molecules is slowed down. The particle size and shell thickness of such silica coated particles are commonly determined by complementing SEM based CLEM with TEM.

The first application of SEM based CLEM to investigate metal NP catalysts was achieved by Zhou *et al.*[33] Catalytic activity mapping of Au nanorods (NR) incorporated into a mesoporous SiO_2 shell was performed by using the oxidative deacetylation of amplex red. Registration of the nanoscale activity maps with the SEM images was ingeniously enabled by using the NR's as fiducial markers. This revealed a heterogeneous activity distribution at the sub-particle level, characterized by an increased activity on the tips compared to the center of the particles (Figure 2). This behavior was less pronounced for larger NR's and, interestingly, a small fraction of NR's showed an opposite behavior. This information would have been lost in ensemble catalytic activity testing.

The heterogeneous activity distribution was attributed to a varying density of crystallographic defects within individual NR's. Such defects, typically low-coordination metal sites, lead to an increased catalytic activity and are more commonly encountered on NR tips compared to sides.[3,4] This corroborates with the notion of locally increased activity. On the other hand, a decreasing activity is observed when probing from the center of the particles towards the tips and this is even more pronounced for larger particles (Figure 2e). This trend is attributed to the presence of growth induced defects on the NP's sides. An increased growth rate induces more surface defects and as the growth rate decreases in time, less defects will be incorporated towards the tips of the particle. Additionally, the synthesis of larger particles is characterized by a relatively large initial growth rate, aggravating the effect. The authors conclude that identifying the surface facets of nanocatalysts is insufficient for correlating with and predicting their reactivity; rather, surface defects can play dominant roles in determining surface reactivity.

The same fluorogenic reaction has been applied by Shen *et al.* to investigate the presence of surface reaction intermediates on mesoporous SiO_2 coated and bare pseudospherical Au NR's.[34] By correlatively applying SEM and SRFM, a surface-adsorbed, one-electron-oxidized amplex red radical intermediate was identified. Based on the reaction kinetics, a heterogeneous activity distribution was observed within the individual NR's which was attributed to the large structural complexity. The presence of this reaction intermediate would thus have remained hidden in ensemble-averaged experiments.

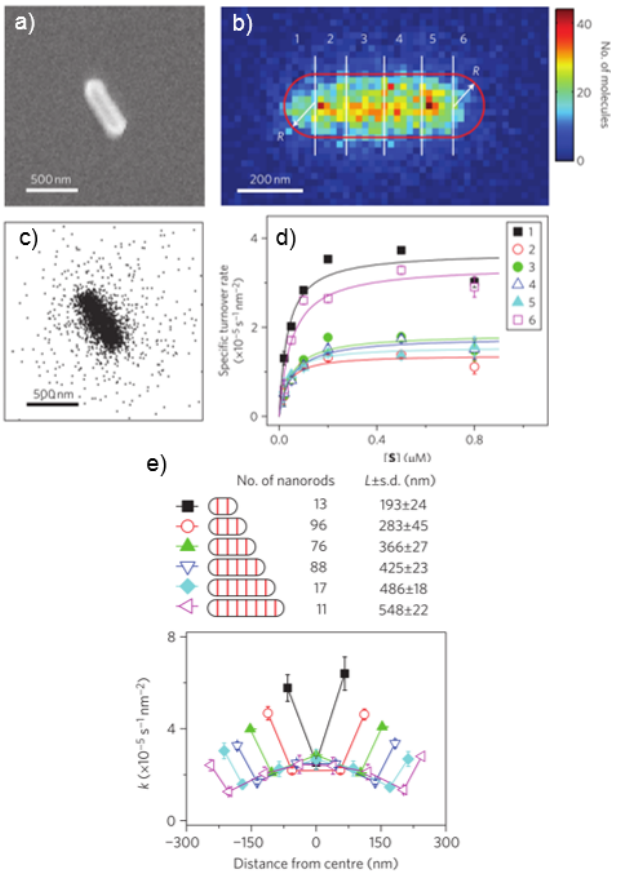

Figure 2. a) SEM image of the Au nanorod particle under investigation. b) Nanoscale catalytic activity map obtained by rotating the image to orient it horizontally and by binning the catalytic turnovers, in 20 x 20 nm^2 areas. The color scale represents the number of turnovers detected in the respective areas, the red line shows the outline of the SiO_2 shell of the nanorod and the white lines subdivide the nanoparticle into six different segments. c) Scatter plot of the first portion of the detected fluorescent product molecules resulting from the catalytic conversion on the Au nanorod represented in a). d) The specific reaction rates of the different segments assigned in b), depending on the fluorogenic reagent concentration. e) The specific catalytic reaction rates within the different sub segments are represented with respect to their distance from the center of the NR's. Averaged data, obtained over 301 nanorods, subdivided into six length groups. The subdivision is shown in the scheme at the top. Adapted with permission from ref. [33]

Such correlative research has also been performed on Au nanoplates with a mesoporous SiO_2 shell using the fluorogenic resazurin to resorufin reduction.[35] A heterogeneous activity distribution was observed on the sub-particle level, showing differences between facets, morphological features and even between the center of a NP and its periphery (Figure 3). More precisely, NP corners proved to be more catalytically active than

edges and even more so than the flat facets, and the activity decreases between the particle's center and edge. The extent of this radially decreasing reactivity was shown to be size dependent, as the effect was less pronounced for larger particles. This is ascribed to the slower growth rate reduction that enables the formation of larger NP's. However, the average specific activity is smaller for larger NP's. These results were interpreted as originating from growth-induced surface defects, as was previously the case for Au NR structures.[33,34]

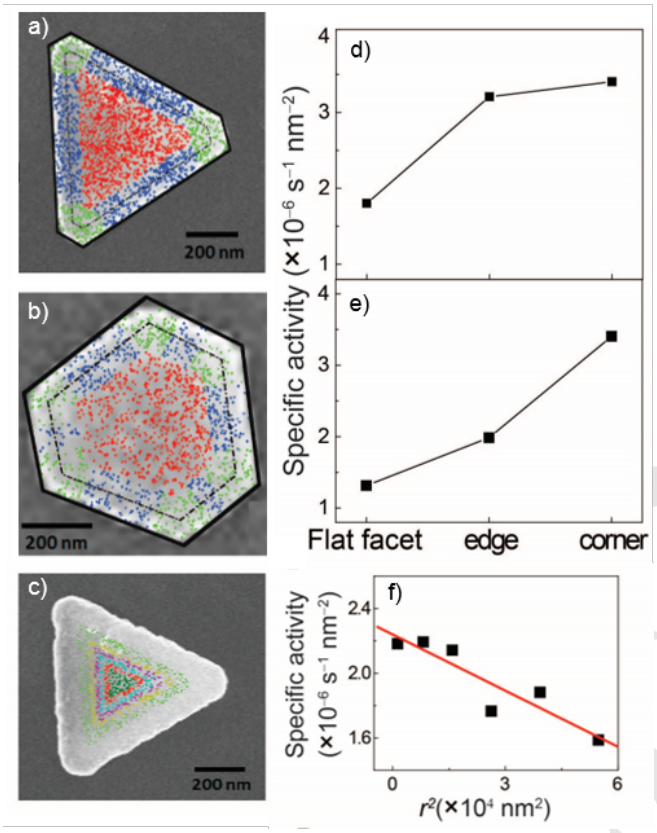

Figure 3. Catalytic activity distribution on the different facets of a) triangular and b) hexagonal Au nanoplates in a SiO_2 shell. Color coding represents the respective regions in which the turnover occurred; flat facet (red), edge (blue) and corner (green). The dashed line highlights the transition between the Au nanoplate and the surrounding SiO_2 shell. c) The specific activity on the different regions of the triangular nanoplate and d) on the hexagonal nanoplate. e) The radial activity gradient on the flat facet. This facet is subdivided into different radial segments towards the outside and color coded. f) Specific activity measured within the different radial segments, where r is the distance between the center of the flat surface and the middle of the corresponding radial segment. Adapted with permission from ref. [35]

Metal NP catalyst samples feature an inter- and intraparticle heterogeneity. Regardless of this heterogeneity, correlative SRFM and SEM has the power to look beyond the ensemble level and reveal sub-particle activity distributions. This enables parallel catalyst screening as a means of high-throughput characterization.[36] As such, highly active catalyst particles can be identified and subpopulations can be easily resolved (Figure 4). It has furthermore been proven that the relevance of these fluorescence-based investigations can be extended towards more generally applied, non-fluorescent catalytic reactions by establishing a correlation between them.[36]

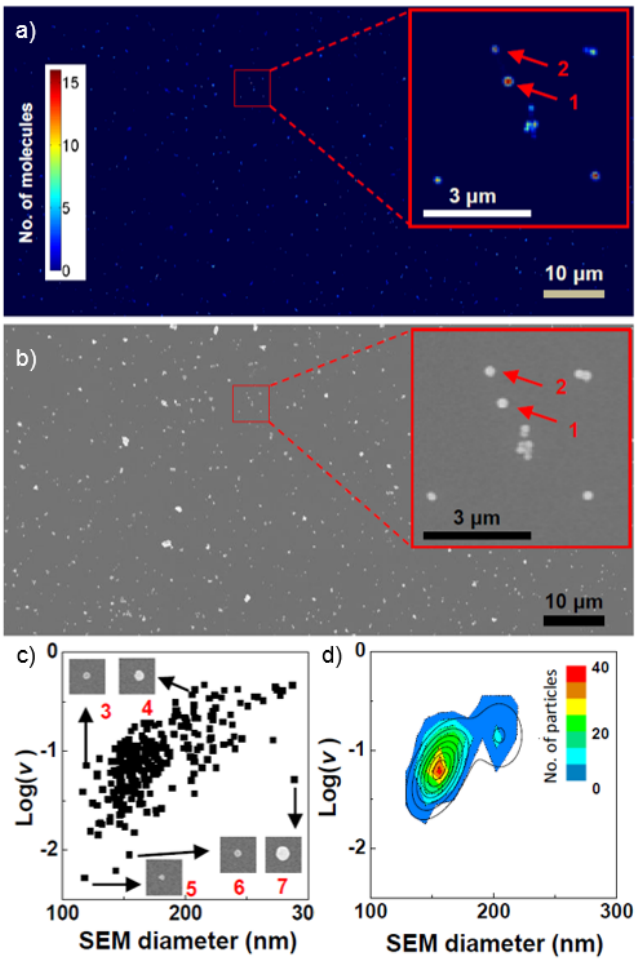

Figure 4. a) Super-resolved catalytic activity map showing the resazurin to resorufin reduction of approximately 1000 pseudospherical gold nanoparticles in a SiO_2 shell. The inset represents a zoomed-in area. b) The corresponding SEM image of the activity map shown in a). c) Scatter plot that shows the turnover rate ($[\nu] = s^{-1}.particle^{-1}$) of individual catalyst particles in function of their diameter and d) contour plot of the histogram in c). The solid black lines represent fits with 2D Gaussian functions. Adapted with permission from ref. [36]

3.2 Nanoscale structure-activity investigation of photocatalysts

Similar to metal NP catalysis, most photocatalytic materials consist of non-porous semiconductor particles in which the activity is limited to the outer crystal surface and crystallographic features play an important role in the photocatalytic performance.[37,38] For example, structural defects can act as electron or hole traps and locally enhance photoreductive or -oxidative activity. Correlative SRFM and SEM is therefore ideally suited to reveal the structure-activity relationship of individual

photocatalyst particles. The function of the optical microscope in such investigations is twofold. Besides enabling catalytic activity mapping by visualizing single conversions of fluorogenic substrates, the optical microscope can also be used to introduce the light that stimulates the photocatalytic process and enables the generation of charge carriers.

Tachikawa *et al.* have developed a redox-responsive fluorogenic probe reaction based on the photoreductive conversion of 3,4-dinitrophenyl-substituted boron dipyrromethene (DN-BODIPY).[39] Using this fluorogenic reaction an increased photoreductive activity on the {101} facets of anatase TiO_2 crystals compared to the {001} facets was revealed.[40] By immobilizing the sample on a cover slide equipped with a numbered grid, SRFM investigations were performed in a specialized inverted sample cell and correlated with SEM. As such, an increased catalytic activity could be attributed to micron scale structural defects. In another experiment, the visible-light photocatalytic activity of Au-NP functionalized TiO_2 was observed to preferentially occur in zones of tens of nanometer surrounding the Au NP deposits.[41] This was assumed to be the result of the local effect of the plasmon-induced electron and/or energy transfer processes.

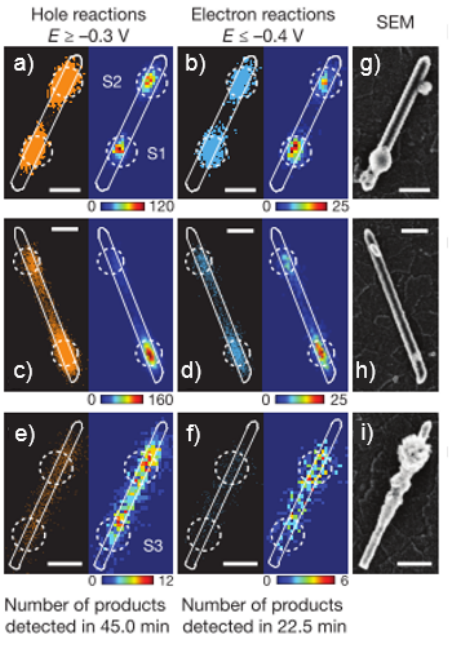

Figure 5. a) Scatter plot (left) and two-dimensional histogram (40 × 40 nm2 pixels; right) of all individual resorufin product molecules (orange dots) generated from hole-induced amplex red oxidation reactions at E ≥ −0.3 V on a single TiO2 nanorod with two localized hotspots. The solid white line is the outline of the nanorod, determined using SEM. Dashed white circles denote focused 375-nm laser spots for photocurrent measurements and OEC deposition. The color scales indicate number of products formed. b) Same as a), but at E ≤ −0.4 V, and the blue dots are resorufin product molecules generated from electron-induced resazurin reduction reactions. c)–f), Same as a) and b), but for a nanorod with a single dominant hole reaction hotspot (c, d) or delocalized hole reactions (e, f). g)–i), SEM images of the three nanorods in a)–f) after OEC deposition. All scale bars are 400 nm. Adapted with permission from ref. [42]

The previously applied amplex red based fluorogenic reaction has also been used to study the photoelectrocatalytic oxidation reaction on rutile TiO_2 particles.[43] In these experiments, an ITO functionalized cover slide was used as cathode to selectively drain the photogenerated electrons. This ensured that electron-induced oxidation pathways were suppressed. Hence, only direct and indirect photooxidation processes, induced by photogenerated holes, were probed. This research proposed a mechanism in which reagent molecules are oxidized by surface-adsorbed hydroxyl radical species and correlative imaging showed a significant inter- and intraparticle heterogeneity. These rutile TiO_2 particles are commonly modified with an oxygen evolution catalyst (OEC) to improve water oxidation efficiency (Figure 5).[42] Correlative SRFM and SEM indicated that careful control over the OEC deposition is important to attain optimal performance. Based on these results, the authors suggested a block-deposit-remove strategy that allows OEC deposition at the preferred positions. Hence, a rational design of catalytic photoelectrodes is within reach.

Reagent adsorption is an important step during photocatalysis and needs to be well understood. The adsorption ability of anatase TiO_2 particles has been investigated using the fluorogenic catechol-modified BODIPY (CA-BODIPY) molecules.[44] As such, a facet and solvent-dependent adsorption was observed, which was indicative for the adsorption of water and organic compounds. The latter were additionally found to be mutually competitive. Additionally, TiO_2 nanocrystals showed an improved adsorption over micrometer-sized particles due to the presence of crystallographic defects. Similarly, an increased exposure of Fe sites near branch tips of Fe_2O_3 pine tree shaped structures also led to a preferred adsorption (Figure 6).

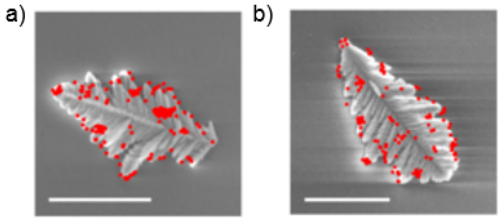

Figure 6. Scatter plots representing the locations of the reactive sites (red dots) on Fe_2O_3 branches determined by means of the fluorogenic CA-BODIPY reaction. A preferential adsorption near branch tips is observed. Scale bars are 2 µm. Adapted with permission from ref. [44]

3.3 Nanoscale structure-activity investigation of solid acid catalysts

The catalytic activity of various zeolite-based acid catalysts has been studied using SRFM. In contrast to metal NP- and photocatalysts, the performance of zeolites originates from the presence of active (acid) sites contained inside the characteristic crystalline, microporous framework. Since these pores typically have similar dimensions as reagent and product molecules, such materials are in high demand for shape selective catalysis.

However, these micropores also induce mass-transport limitations.[45] This is commonly resolved by introducing meso- and macroporous defects to enhance catalytic performance. Such introductions bring variability inside the crystalline zeolite framework. Furthermore, for industrial scale applications, these zeolite catalysts are often embedded in large catalyst bodies, such as extrudates. During the shaping of these catalysts, various chemicals are added into the system that can alter the catalytic performance via pore blocking and de- and realumination.[46,47] Resulting catalyst performance is then affected by all these numerous factors – porosity, framework variability,

The first correlative structure-activity investigation in the field of zeolite catalysis was achieved by Karreman *et al.* By using an ILEM that combined TEM and CLSM, the catalytic activity distribution in fluid catalytic cracking (FCC) particles was studied.[48,49] However, the specific system configuration and required sample slicing prohibited nanoscale catalytic activity mapping (Figure 1c). The researchers therefore prestained the catalytic domains using the fluorogenic 4-fluorostyrene oligomerization reaction. Zeolite catalysts allow such a staining, as the active sites are confined within a microporous structure. Local Brønsted acidity was thus revealed based on the fluorescence intensity obtained by diffraction limited CLSM and could directly be related to the structural organization of the FCC particles as observed by TEM. This revealed a heterogeneous distribution of the zeolite and matrix material within the FCC particles and after applying hydrothermal deactivation to mimic different life stages of the FCC catalyst, both structural and activity changes were observed.

More recently, our group was the first to investigate solid acid zeolite catalysts using correlative SRFM and EM (Figure 7).[50,51] By applying an integrated light and electron microscope with SRFM capabilities, time-consuming sample transfer became obsolete. However, as the nanoscale catalytic activity mapping required a liquid phase fluorogenic reagent, a consecutive approach was still needed, performing structural imaging prior to venting the SEM chamber and adding the furfuryl alcohol reagent. This research directly revealed unanticipated catalytic activity on inter-particle intergrowth structures in a small-port mordenite sample. By applying linear polarized excitation light, the orientation of the formed product molecules could furthermore be correlated to the direction of the one dimensional porous structure,[52] indicating that catalytic activity mainly originates from active sites within the microporous structure and contributes to shape selectivity. Additionally, the effect of dealumination by acid leaching was demonstrated to be limited to the initially active regions. These observations contrast with Raman microscopy studies using pyridine as acid probe. Based on the latter, which resembles traditional bulk scale FTIR investigations, the full catalyst particle was shown to be accessible for organic molecules. This discrepancy was ascribed to the dynamic nature of the SRFM investigations, including information on mass transport within the microporous structure, and indicates the relevance of correlative structure-activity investigations, as this information is lost in bulk scale experiments.

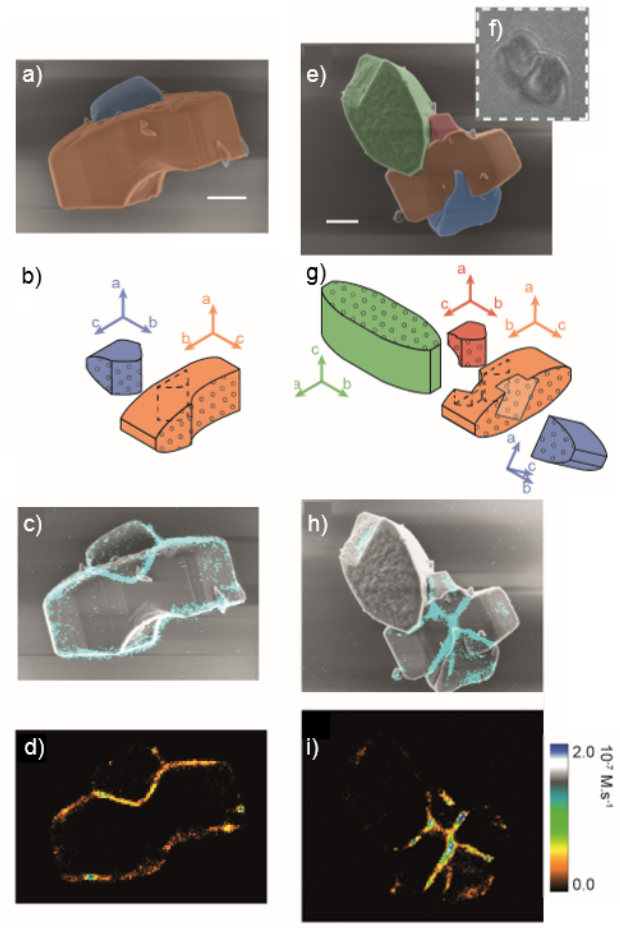

Figure 7.: a, e) Pseudo-colored scanning electron micrographs of intergrown crystallites. b, g) The corresponding schematic representations with an indication of the different crystallographic axes. The (001) facets, where the 12MR channels surface, are marked by the dotted pattern indicating the 12MR pore entrances. c, h) Overlay images of the detected individual fluorescent products (cyan dots) on the scanning electron micrographs. d, i) The quantitative NASCA images obtained by binning the turnovers in 50 x 50 nm^2 zones. (f) Optical transmission image of the second aggregate. Scale bars: 1 µm. Adapted with permission from ref. [50]

3. Conclusion and perspectives

Correlative SRFM and SEM has been successfully applied in (photo)catalytic research to unravel the effects of intrinsically complex catalyst structures on its performance. By linking nanoscale catalytic activity maps to the local structural context, pronounced inter- and intraparticle activity distributions were revealed for every reported catalyst sample. These insights went unnoticed using traditional catalyst characterization techniques as they are often the result of minute sub-particle structural features and defects. The reported correlative experiments were mainly performed on dedicated setups; however, more recent research resulted from the application of an integrated light and electron microscopes. Such approaches have the potential to accelerate research into the local, small-scale structure-activity relationship

of heterogeneous catalysts, as it decreases sampling time and increases accuracy.

It is expected that even more in depth insights will come from future technical developments. For example, the application of a liquid cell will enable *in situ* SEM imaging of (photo)catalysts during fluorogenic-reaction-based catalytic activity mapping and could enable catalytic activity mapping at elevated temperatures and pressures. This is highly relevant, as the catalyst working mechanisms are strongly influenced by reaction conditions. Additionally, the SRFM axial resolution could be further increased as this resolution is currently still diffraction-limited. Crucial depth information is therefore lost and lateral nanoscale details are obscured as information of different structural origins is superimposed. The recent advent of 3D SRFM techniques would thus further increase the resolving power of nanoscale catalytic activity maps.[53,54] Finally, given the complexity of heterogeneous catalysts, the structure-activity information should further be complemented with insights into other aspects related to catalysis. This is available by the application of complementary techniques such as Raman microscopy or elemental analysis. Ultimately, correlative structure-activity investigations will lead to a more rationalized catalyst synthesis as the availability of an accurate structure-activity relationship can serve as the starting point for the development of improved catalyst samples. This might further be facilitated by high-throughput catalyst preparation.

Acknowledgements

The authors gratefully acknowledge financial support from the Research Foundation-Flanders (FWO, G.0962.13, Hercules AKUL/11/14), KU Leuven Research Fund (C14/15/053, OT/12/059), and the European Research Council under the European Union's Seventh Framework Programme (FP/2007-2013) / ERC Grant Agreement no. [307523], ERC-Stg LIGHT to M.B.J.R.

Keywords: Heterogeneous catalysis • Photocatalysis • Structure-activity relationships • Super-resolution fluorescence microscopy• Electron microscopy

[1] D. Olaf, K. Helmut, K. Karl, T. Thomas, in *Ullmann's Encycl. Ind. Chem.* (Ed.: M. Bohnet), John Wiley And Sons, **2014**, pp. 457–481.

[2] E. G., K. H., W. J., Eds. , *Handbook of Heterogeneous Catalysis*, Wiley-VCH, **1997**.

[3] G. A. Somorjai, L. Yimin, *Introduction to Surface Chemistry and Catalysis*, Wiley, **2010**.

[4] G. Ertl, *Reactions at Solid Surfaces*, Wiley, **2009**.

[5] D. Astruc, Ed. , *Nanoparticles and Catalysis*, Wiley-VCH, **2008**.

[6] M. R. Hoffmann, S. T. Martin, W. Choi, D. W. Bahnemannt, **1995**, 69–96.

[7] X. Chen, S. S. Mao, **2007**.

[8] J. Cejka, A. Corma, S. Jones, Eds. , *Zeolites and Catalysis: Synthesis, Reactions and Applications*, Wiley-VCH, **2010**.

[9] J. Hagen, Ed. , *Industrial Catalysis: A Practical Approach*, Wiley-VCH, **2006**.

[10] T. Franklin, Ed. , *Metal Nanoparticles for Catalysis: Advances and Applications*, The Royal Society Of Chemistry, **2014**.

[11] D. A. King, P. D. Woodruff, Eds. , *The Chemical Physics of Solid Surfaces and Heterogeneous Catalysis, Vol. 4*, **1982**.

[12] T. Cordes, S. A. Blum, *Nat. Publ. Gr.* **2013**, *5*, 993–999.

[13] P. Chen, X. Zhou, N. M. Andoy, K.-S. Han, E. Choudhary, N. Zou, G. Chen, H. Shen, *Chem. Soc. Rev.* **2014**, *43*, 1107–1117.

[14] K. P. F. Janssen, G. De Cremer, R. K. Neely, A. V Kubarev, J. Van Loon, J. a Martens, D. E. De Vos, M. B. J. Roeffaers, J. Hofkens, *Chem. Soc. Rev.* **2014**, *43*, 990–1006.

[15] I. L. C. Buurmans, B. M. Weckhuysen, *Nat. Chem.* **2012**, *4*, 873–886.

[16] B. M. Weckhuysen, *Chem. Soc. Rev.* **2010**, *39*, 4557–4559.

[17] W. Wang, J. Gu, T. He, Y. Shen, S. Xi, L. Tian, F. Li, H. Li, L. Yan, X. Zhou, *Nano Res.* **2015**, *8*, 441–455.

[18] M. B. J. Roeffaers, B. F. Sels, H. Uji-I, F. C. De Schryver, P. a Jacobs, D. E. De Vos, J. Hofkens, *Nature* **2006**, *439*, 572–575.

[19] K. Naito, T. Tachikawa, M. Fujitsuka, T. Majima, *J. Phys. Chem. C* **2008**, *112*, 1048–1059.

[20] W. Xu, J. S. Kong, Y.-T. E. Yeh, P. Chen, *Nat. Mater.* **2008**, *7*, 992–996.

[21] D. Wöll, C. Flors, *Small Methods* **2017**, 1700191–1700203.

[22] M. B. J. Roeffaers, G. De Cremer, J. Libeert, R. Ameloot, P. Dedecker, A. J. Bons, M. Bückins, J. A. Martens, B. F. Sels, D. E. De Vos, et al., *Angew. Chemie - Int. Ed.* **2009**, *48*, 9285–9289.

[23] G. De Cremer, B. F. Sels, D. E. De Vos, J. Hofkens, M. B. J. Roeffaers, *Chem. Soc. Rev.* **2010**, *39*, 4703–4717.

[24] T. Tachikawa, S. Yamashita, T. Majima, **2011**, 7197–7204.

[25] B. M. Weckhuysen, *Angew. Chemie - Int. Ed.* **2009**, *48*, 4910–4943.

[26] J. B. Sambur, P. Chen, *Annu. Rev. Phys. Chem.* **2014**, *65*, 395–422.

[27] A. V. Kubarev, K. P. F. Janssen, M. B. J. Roeffaers, *ChemCatChem* **2015**, *7*, 3646–3650.

[28] B. G. Kopek, M. G. Paez-segala, G. Shtengel, K. A. Sochacki, M. G. Sun, Y. Wang, C. S. Xu, S. B. Van Engelenburg, J. W. Taraska, L. L. Looger, et al., *Nat. Publ. Gr.* **2017**, *12*, 916–946.

[29] P. de Boer, J. P. Hoogenboom, B. N. G. Giepmans, *Nat. Methods* **2015**, *12*, 503–513.

[30] A. V. Agronskaia, J. A. Valentijn, L. F. van Driel, C. T. W. M. Schneijdenberg, B. M. Humbel, P. M. P. van Bergen en Henegouwen, A. J. Verkleij, A. J. Koster, H. C. Gerritsen, *J. Struct. Biol.* **2008**, *164*, 183–189.

[31] A. C. Zonnevylle, R. F. C. Van Tol, N. Liv, A. C. Narvaez, A. P. J. Effting, P. Kruit, J. P. Hoogenboom, *J. Microsc.* **2013**, *252*, 58–70.

[32] E. Debroye, J. Van Loon, X. Gu, T. Franklin, J. Hofkens, K. P. F. Janssen, M. B. J. Roeffaers, *Part. Part. Syst. Charact.* **2016**, *33*, 412–418.

[33] X. Zhou, N. M. Andoy, G. Liu, E. Choudhary, K.-S. Han, H. Shen, P. Chen, *Nat. Nanotechnol.* **2012**, *7*, 237–241.

[34] H. Shen, X. Zhou, N. Zou, P. Chen, *J. Phys. Chem. C* **2014**, *118*, 26902–26911.

[35] N. M. Andoy, X. Zhou, E. Choudhary, H. Shen, G. Liu, P. Chen, *J. Am. Chem. Soc.* **2013**, *135*, 1845–1852.

[36] X. Zhou, E. Choudhary, N. M. Andoy, N. Zou, P. Chen, *ACS Catal.* **2013**, *3*, 1448–1453.

[37] R. Li, F. Zhang, D. Wang, J. Yang, M. Li, J. Zhu, X. Zhou, H. Han, C. Li, *Nat. Commun.* **2013**, *4*, 1432.

[38] E. Debroye, J. Van Loon, H. Yuan, K. P. F. Janssen, Z. Lou, S. Kim, T. Majima, M. B. J. Roeffaers, *J. Phys. Chem. Lett.* **2017**, *8*, 340–346.

[39] T. Tachikawa, N. Wang , S. Yamashita, S.-C. Cui, T. Majima, *Angew. Chemie Int. Ed.* **2010**, *49*, 8593–8597.

[40] T. Tachikawa, S. Yamashita, T. Majima, *J. Am. Chem. Soc.* **2011**, *133*, 7197–7204.

[41] T. Tachikawa, T. Yonezawa, T. Majima, *ACS Nano* **2013**, *7*, 263–275.

[42] J. B. Sambur, T.-Y. Chen, E. Choudhary, G. Chen, E. J. Nissen, E. M. Thomas, N. Zou, P. Chen, *Nature* **2016**, *530*, 77–80.

[43] J. B. Sambur, P. Chen, *J. Phys. Chem. C* **2016**, *120*, 20668–20675.

[44] T. Tachikawa, T. Ohsaka, Z. Bian, T. Majima, *J. Phys. Chem. C* **2013**.

[45] G. De Cremer, E. Bartholomeeusen, P. P. Pescarmona, K. Lin, D. E. De Vos, J. Hofkens, M. B. J. Roeffaers, B. F. Sels, *Catal. Today* **2010**, *157*, 236–242.

[46] N. Michels, S. Mitchell, J. Pérez-Ramirez, *ACS Catal.* **2014**, *4*, 2409–2417.

[47] G. T. Whiting, A. D. Chowdhury, R. Oord, P. Paalanen, B. M. Weckhuysen, *Faraday Discuss.* **2016**, *188*, 369–386.

[48] M. A. Karreman, I. L. C. Buurmans, J. W. Geus, A. V. Agronskaia, J. Ruiz-Martínez, H. C. Gerritsen, B. M. Weckhuysen, *Angew. Chemie - Int. Ed.* **2012**, *51*, 1428–1431.

[49] M. A. Karreman, I. L. C. Buurmans, A. V. Agronskaia, J. W. Geus, H. C. Gerritsen, B. M. Weckhuysen, *Chem. - A Eur. J.* **2013**, *19*, 3846–3859.

[50] J. Van Loon, K. P. F. Janssen, T. Franklin, A. V Kubarev, J. A. Steele, E. Debroye, E. Breynaert, J. A. Martens, M. B. J. Roeffaers, *ACS Catal.* **2017**, *7*, 5234–5242.

[51] K. Kennes, C. Demaret, J. Van Loon, A. V. Kubarev, G. Fleury, M. Sliwa, O. Delpoux, S. Maury, B. Harbuzaru, M. B. J. Roeffaers, *ChemCatChem* **2017**, *9*, 3440–3445.

[52] K. L. Liu, A. V. Kubarev, J. Van Loon, H. Uji-I, D. E. De Vos, J. Hofkens, M. B. J. Roeffaers, *ACS Nano* **2014**, *8*, 12650–12659.

[53] B. Huang, W. Wang, M. Bates, X. Zhuang, *Science (80-.).* **2008**, *319*, 810–813.

[54] B. Huang, J. Sara, B. Brandenburg, X. Zhuang, *Nat. Methods* **2008**, *5*, 1047–1052.

WILEY-VCH

Entry for the Table of Contents (Please choose one layout)

FOCUS REVIEW

A thorough understanding of the catalyst structure-activity relationship at the smallest possible length scales is required for intelligent catalysts improvement. Such nanometer resolved investigations are enabled by combined fluorescence and electron microscopy. Here, we discuss different experimental approaches and insights obtained through their application.

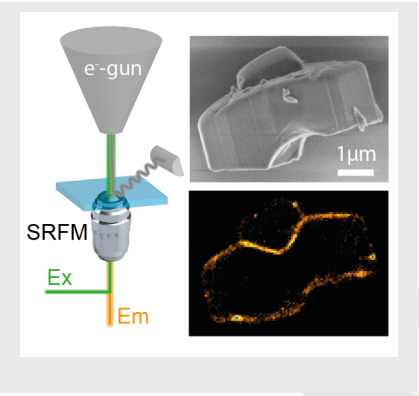

*Jordi Van Loon, Alexey V. Kubarev, and Maarten B. J. Roeffaers**

Page No. – Page No.

Correlating catalyst structure and activity at the nanoscale

WILEY-VCH

FOCUS REVIEW

Additional Author information for the electronic version of the article.

Jordi Van Loon: 0000-0001-5189-7805
Alexey V. Kubarev: 0000-0001-8327-0345
Maarten B.J. Roeffaers: 0000-0001-6582-6514